Thermodynamic nature of the antiferromagnetic transition in Na_xCoO_2

C. A. M. dos Santos,[1,2] J. J. Neumeier,[1] Yi-Kuo Yu,[3] R. K. Bollinger,[1] R. Jin,[4] D. Mandrus,[4] and B. C. Sales[4]
[1]*Department of Physics, P.O. Box 173840, Montana State University, Bozeman, Montana 59717-3840, USA*
[2]*Escola de Engenharia de Lorena-USP, P.O. Box 116, Lorena, SP 12602-810, Brazil*
[3]*National Center for Biotechnology Information, 8600 Rockville Pike, Bethesda, Maryland 20894, USA*
[4]*Material Science and Technology Division, Oak Ridge National Laboratory, Oak Ridge, Tennessee 37831-6056, USA*
(Received 26 May 2006; revised manuscript received 26 July 2006; published 3 October 2006)

High-resolution thermal expansion measurements of single-crystalline $Na_{0.80}CoO_2$ reveal continuous behavior of the paramagnetic-antiferromagnetic phase transition at $T_M=21.7(1)$ K with critical exponent $\alpha=0.18(2)$. The thermal expansion is found to be highly anisotropic. Thermodynamic analysis provides the hydrostatic pressure derivative $dT_M/dP=+4.6(2)$ K/GPa. Similar measurements and analysis are presented for $Na_{0.75}CoO_2$.

DOI: 10.1103/PhysRevB.74.132402 PACS number(s): 75.40.Cx, 65.40.−b, 65.40.De, 65.40.Ba

The compound Na_xCoO_2 exhibits intriguing magnetic and transport properties.[1–7] Intercalation with water induces superconductivity[8–10] with critical temperature T_c near 5 K for $Na_{0.3}CoO_2\cdot 1.4H_2O$. Despite the relatively low T_c, this compound offers a new window into the study of transition-metal oxide superconductivity because of similarities to the (high-T_c) cuprate superconductors including an anisotropic structure consisting of transition-metal ion/oxygen layers and a compositional phase diagram where antiferromagnetism resides nearby to superconductivity.[10] Although the antiferromagnetic ordering temperature, $T_M\sim 22$ K, is low compared to that of the cuprates,[4,7,8,10–12] it has been suggested that spin fluctuations mediate the superconductivity.[9,13,14] For these reasons, determining the fundamental nature of this antiferromagnetism is important since it will constrain theoretical models.

Herein two questions are addressed regarding the thermodynamic nature of the antiferromagnetic phase transition of Na_xCoO_2. (1) Is the transition continuous (second order) and (2) if so, what is the magnitude of the critical exponent α associated with the specific heat? To answer these questions, high-resolution thermal expansion and heat capacity measurements are utilized. Simultaneous application of these techniques can establish whether or not a phase transition is continuous[15] and reveal anisotropies associated with the phase transition. In addition, the extremely high relative resolution of our thermal expansion technique[15,16] reveals new details about the general physical behavior of Na_xCoO_2.

The single crystals, grown by the optical float-zone method, have lattice parameters $a=2.83$ Å, $c=10.88$ Å ($x=0.75$) and $a=2.83$ Å, $c=10.84$ Å ($x=0.80$), consistent with published values.[5–7,17] Heat capacity and dc-magnetization measurements were performed using a Quantum Design Physical Properties Measurement System. A fused-quartz dilatometer[16] was used to measure linear thermal expansion along the a and c axes; it can detect 0.1 Å length changes. Thermal expansion is measured on warming from 6 K at a rate of 0.20(1) K/min; for the present data, the samples were cooled at less than 1.1 K/min. In the course of this study, thermal expansion was measured along each axis on two separate crystals removed from the $x=0.80$ single crystal boule; one of these was measured twice. One $x=0.75$ crystal was measured; its thermal expansion was measured three times along each axis. In all of these measurements, the features discussed below reproduced well. The $x=0.75$ and 0.80 crystals used to acquire the data shown below had thicknesses of 1.342 and 1.191 mm (a axis), and 2.329 and 1.015 mm (c axis), respectively.

Magnetic susceptibility χ vs temperature was measured with field parallel to the a and c directions. The data (not shown) display signatures of antiferromagnetic ordering at $T_M=21.8(2)$ K for both samples. Above T_M, χ decreases with increasing temperature and is approximately field independent indicating a paramagnetic state. Other reports[2,3] agree with our measurements. Linear behavior is observed in χ^{-1} vs temperature ($50\ \text{K}<T<200\ \text{K}$) for the a and c directions. Using the Curie-Weiss law [$\chi=C/(T-\Theta)$, C is the Curie constant], it was possible to determine Θ from the a axis data as −251 and −257 K and the c axis data as −149 and −195 K for $x=0.75$ and 0.80, respectively. Negative Θ values are consistent with antiferromagnetic order[2,18] below T_M. The large magnitude of the Θ values indicate a high degree of Na order.[18]

Heat capacity at constant pressure C_P (insets of Fig. 1) for $x=0.80$ and 0.75 clearly reveals the antiferromagnetic transition at T_M. The absolute values of $C_P(T)$ are of the same magnitude as reported previously.[2,3,18] Our high-resolution linear thermal expansion results are shown in Fig. 1 where $\Delta L/L_{300\ \text{K}}$ is plotted for the a and c directions. The shrinkage along c is one order of magnitude larger than along a in the temperature range $6\ \text{K}<T<300\ \text{K}$. This anisotropy is common in layered hexagonal structures[16,20,21] which are significantly stiffer along the a direction. An interesting feature occurs around 220 K in both the a and c axes (the feature is most prominent in the c axis data of the $x=0.75$ sample). This effect seems correlated with the deviation of the Curie-Weiss law above ~200 K. Its origin may be related to Na-ion mobility as reported by others.[4,5,17,18] We found that cooling our samples at rates higher than 1.1 K/min had a strong influence on this feature in the $x=0.75$ sample, suggesting that it is first-order in nature.

Figure 2 highlights the behavior of $\Delta L/L_{300\ \text{K}}$ in the vicinity of T_M. Distinct changes in slope resulting from the paramagnetic-antiferromagnetic phase transition occur at T_M.

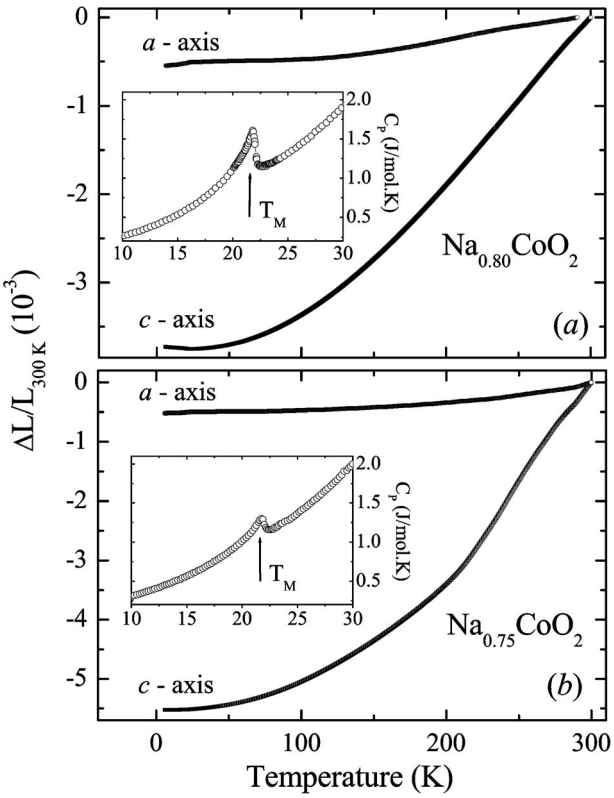

FIG. 1. Linear thermal expansion $\Delta L/L_{300\ \mathrm{K}}$ for (a) $Na_{0.80}CoO_2$ and (b) $Na_{0.75}CoO_2$. Insets show C_P near T_M.

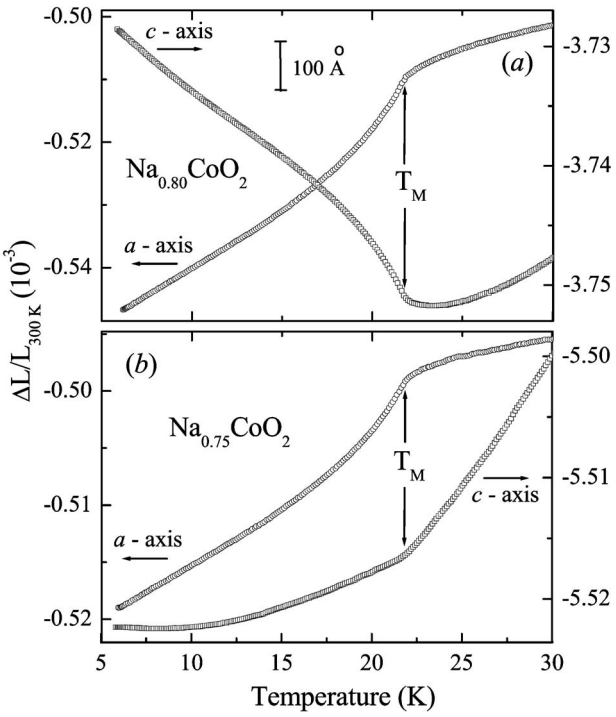

FIG. 2. $\Delta L/L_{300\ \mathrm{K}}$ near T_M for (a) $Na_{0.80}CoO_2$ and (b) $Na_{0.75}CoO_2$. The 100 Å scale indicates the *absolute* length change along a for our 2.329 mm $Na_{0.80}CoO_2$ sample.

These thermal expansion data possess more than four orders of magnitude higher *relative* resolution than thermal expansion data from x-ray or neutron diffraction.[19] They are raw data, corrected for the thermal expansion of fused quartz,[16] with no other processing or averaging. The 100 Å bar in the upper panel of Fig. 2 illustrates this resolution; it represents an *absolute* length scale for the 2.329 mm long sample along a and reveals the Å-scale resolution.

Figure 3(a) shows the linear (μ_a and μ_c) and volumetric (Ω) thermal expansion coefficients for $x=0.80$ near T_M. They were obtained by differentiating $\Delta L/L_{300\ \mathrm{K}}$ using a method described previously.[16] The volume thermal expansion was calculated through the relation $\Omega=2\mu_a+\mu_c$. The shape of the magnetic phase transition is reminiscent of a λ-transition.[21] A negative μ_c is observed below T_M. Negative thermal expansivities are common in the c direction of layered hexagonal structures.[20,21] The thermal expansion coefficients of the $x=0.75$ crystal [Fig. 3(b)] behave in a similar fashion although the negative thermal expansion along c does not occur near T_M and *slightly* negative values of μ_c occur only below 8 K; the sharpness of the peak in μ_c was influenced by the cooling rate which suggests that Na diffusion among vacancies[5] may affect the magnetic transition in this sample. This effect was not observed in the $x=0.80$ sample.

It is significant that according to the third law of thermodynamics, Ω, μ_a, and μ_c must tend to zero as T approaches zero; the hypothetical behavior is indicated by the dashed lines in Fig. 3 for Ω. Distinct curvature toward zero is visible in our data for $x=0.75$ and 0.80 below ~6.2 K, which coincides with downturns in C_P as reported previously.[18] The

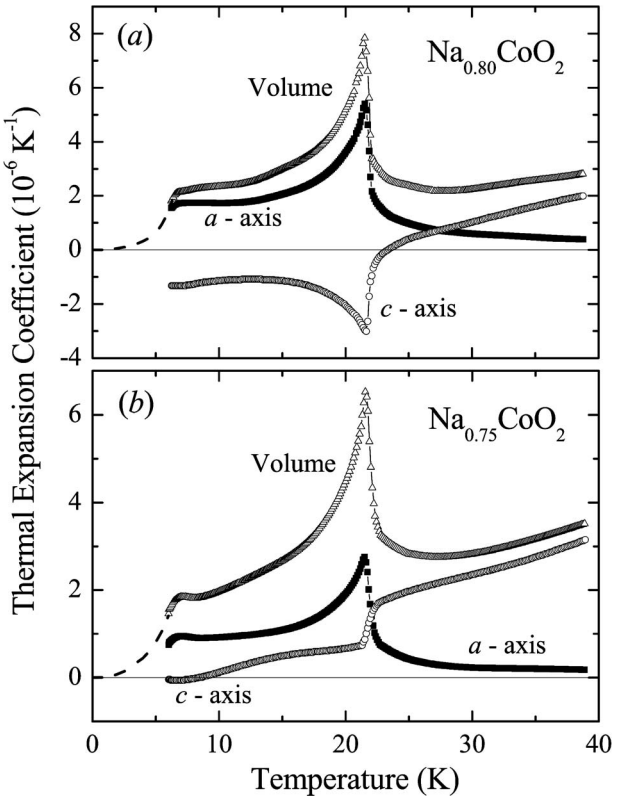

FIG. 3. Linear (μ_a and μ_c) and volume ($\Omega=2\mu_a+\mu_c$) thermal expansion coefficients for (a) $Na_{0.80}CoO_2$ and (b) $Na_{0.75}CoO_2$. Dashed lines (one curve per panel) indicate behavior expected from the third law of thermodynamics.

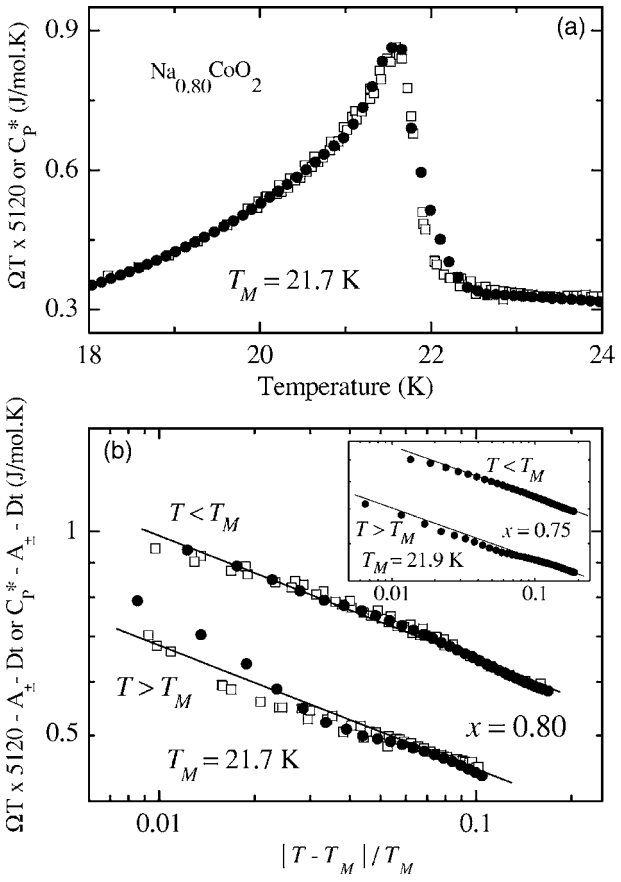

FIG. 4. (a) Overlap of ΩT (closed symbols) and C_P^* (open symbols) for $x=0.80$. (b) The critical behavior above and below T_M using ΩT and C_P^* on a log-log plot. Linear least-squares fitting (solid line) reveals the same exponent $\alpha=0.18(2)$ above and below T_M. The inset shows ΩT (arbitrary scale) for $x=0.75$ which yields $\alpha=0.18(1)$.

physical origin of these features are unclear. Perhaps another phase transition occurs at 6.2 K or this feature might simply be due to a few anomalous phonon modes.

The phase transition's nature is now evaluated using a recently reported thermodynamic approach.[15] According to this method, if ΩT and C_P reveal good overlap after subtraction of a term linear in T from C_P near the phase transition $[C_P^*=C_P-(aT+b)]$, the transition is continuous. The results are shown in Fig. 4(a) for $x=0.80$. Excellent overlap with ΩT in the vicinity of T_M is obtained, thus the paramagnetic-antiferromagnetic phase transition is continuous (second-order). Analysis of the $x=0.75$ crystal also revealed good overlap (not shown) and continuous behavior.

In the vicinity of the phase transition, the one-parameter scaling theory of critical phenomena for continuous phase transitions[15] predicts that C_P^* and ΩT must scale as $\sim|t|^{-\alpha_\pm}$, where $t\equiv(T-T_M)/T_M$, with the same critical exponent above $(+)$ and below $(-)$ T_M. Rather than use a complicated background subtraction, we allow only a subtraction linear in t and two constant shifts $A_\pm$. That is, we assume that when $T>T_M$ $(T<T_M)$, ΩT can be fitted by the expression $A_\pm+(B_\pm/\alpha)|t|^{-\alpha}+Dt$. Making a grid for $0\leqslant A_\pm\leqslant 0.5$, $-1\leqslant D\leqslant 0$ and $21\text{ K}\leqslant T_M\leqslant 22.5$ K and plotting $|t|$ vs $5120\Omega T-A_\pm-Dt$ (or $2297\Omega T-A_\pm-Dt$ for $x=0.75$) on a log-log scale, we choose the set of $A_\pm$, D, and T_M that maximize the power-law fittable temperature range and minimize the deviation within the fitted range ($18\text{ K}<T<24$ K). Using the optimal $A_+=0.20(1)$, $A_-=0.097(5)$, $D=-0.79(4)$, and $T_M=21.7(1)$, C_P^* and scaled ΩT vs t are plotted in Fig. 4(b). Linear least-squares fitting of these data reveals the same exponent $\alpha=0.18(2)$ above and below T_M, thus providing further support that the transition at T_M is continuous. An exponent $\alpha=0.18(1)$ was obtained for the $x=0.75$ specimen using $A_+=0.041(2)$, $A_-=0.081(4)$, $D=-0.25(1)$, and $T_M=21.9(2)$ [see inset of Fig. 4(b)].

The overlap of C_P^* and ΩT is now used to estimate the pressure dependence[15] of T_M with

$$\frac{dT_M}{dP}=\frac{v\Omega T_M}{C_P^*}. \tag{1}$$

Using $\Omega=7.8(2)\times10^{-6}$ K^{-1}, $C_P^*=0.86(2)$ J/mol K, $T_M=21.7(1)$ K, and the specific volume $v=2.32\times10^{-5}$ m^3/mol from our crystallographic data, $dT_M/dP=+4.6(2)$ K/GPa is determined for the sample with $x=0.80$. This result is comparable to $dT_M/dP=+4.4(3)$ K/GPa and $+2.5(2)$ K/GPa for $x=0.70$ and 0.75, respectively.[22,23] Similar analysis for the $x=0.75$ sample $[\Omega=6.6(2)\times10^{-6}$ K^{-1}, $C_P^*=0.33(1)$ J/mol K, and $T_M=21.9(2)$ K] yields $dT_M/dP=+10.0(7)$ K/GPa.

The highly anisotropic nature of the data in Fig. 3 illustrates that the transition into the antiferromagnetic state leads to a strain along c that is opposite to the strain along a. Although similar anisotropic strains in high-T_c superconductors have been used to estimate uniaxial stress (pressure) derivatives,[24] careful analysis must be applied to correctly consider the stress along one axis, the resulting strains and induced stresses along other axes, and how they affect the transition temperature. This analysis requires knowledge of the elastic constants and will be addressed in future work.[25]

The key findings herein are the continuous nature of the antiferromagnetic phase transition and the critical exponents. The critical exponent α is larger than typical for standard antiferromagnets, which have α values closer[26] in magnitude to 0.1. One might associate this difference with the two-dimensionality of Na_xCoO_2 or the triangular Co lattice, which could lead to magnetic frustration.[27,28] However, the A-type structure of Na_xCoO_2 $(0.75\leqslant x\leqslant 0.82)$, with Co magnetic moments oriented parallel to the c axis,[3,12] would be less susceptible to frustration than triangular lattice systems with *in-plane* magnetic moment orientation.[28] On the other hand, the metallic electrical conductivity of Na_xCoO_2 $(0.75\leqslant x\leqslant 0.82)$ leads to ferromagnetic double-exchange within the Co-O planes that coexists with superexchange interactions along the c axis.[14] Thus a more likely scenario is that the large α can be attributed to the simultaneous existence of these distinctly different magnetic exchange interactions. A better understanding of the large observed value of α will help to constrain theoretical models for novel superconducting compounds.

The authors thank J. W. Lynn for valuable discussions. This material is based upon work supported by the Brazilian agency CAPES (0466/05-0), the National Science Foundation (DMR-0504769), the U.S. Department of Energy (DE-FG-06ER46269), and the Division of Materials Sciences and Engineering, U.S. Department of Energy Office of Basic Energy Sciences under Contract No. DE-AC05-00OR22725 with Oak Ridge National Laboratory, managed and operated by UT-Battelle, LLC.

[1] I. Terasaki, Y. Sasago, and K. Uchinokura, Phys. Rev. B **56**, R12685 (1997).
[2] T. Motohashi, R. Ueda, E. Naujalis, T. Tojo, I. Terasaki, T. Atake, M. Karppinen, and H. Yamauchi, Phys. Rev. B **67**, 064406 (2003).
[3] S. P. Bayrakci, C. Bernhand, D. P. Chen, B. Keimer, R. K. Kremer, P. Lemmens, C. T. Lin, C. Niedermayer, and J. Strempfer, Phys. Rev. B **69**, 100410(R) (2004).
[4] M. L. Foo, Y. Wang, S. Watauchi, H. W. Zandbergen, Tao He, R. J. Cava, and N. P. Ong, Phys. Rev. Lett. **92**, 247001 (2004).
[5] R. J. Balsys and R. L. Davis, Solid State Ionics **93**, 279 (1996).
[6] J. W. Lynn, Q. Huang, C. M. Brown, V. L. Miller, M. L. Foo, R. E. Schaak, C. Y. Jones, E. A. Mackey, and R. J. Cava, Phys. Rev. B **68**, 214516 (2003).
[7] Q. Huang, M. L. Foo, R. A. Pascal, Jr., J. W. Lynn, B. H. Toby, Tao He, H. W. Zandbergen, and R. J. Cava, Phys. Rev. B **70**, 184110 (2004).
[8] K. Takada, H. Sakurai, E. Takayama-Muromachi, F. Izumi, R. A. Dilanian, and T. Sasaki, Nature (London) **422**, 53 (2003).
[9] R. Jin, B. C. Sales, P. Khalifah, and D. Mandrus, Phys. Rev. Lett. **91**, 217001 (2003).
[10] C. J. Milne, D. N. Argyriou, A. Chemseddine, N. Aliouane, J. Veira, S. Landsgesell, and D. Alber, Phys. Rev. Lett. **93**, 247007 (2004).
[11] S. P. Bayrakci, I. Mirebeau, P. Bourges, Y. Sidis, M. Enderle, J. Mesot, D. P. Chen, C. T. Lin, and B. Keimer, Phys. Rev. Lett. **94**, 157205 (2005).
[12] L. M. Helme, A. T. Boothroyd, R. Coldea, D. Prabhakaran, D. A. Tennant, A. Hiess, and J. Kulda, Phys. Rev. Lett. **94**, 157206 (2005).
[13] M. D. Johannes, I. I. Mazin, D. J. Singh, and D. A. Papaconstantopoulos, Phys. Rev. Lett. **93**, 097005 (2004).
[14] M. D. Johannes, I. I. Mazin, and D. J. Singh, Phys. Rev. B **71**, 214410 (2005).
[15] J. A. Souza, Yi-Kuo Yu, J. J. Neumeier, H. Terashita, and R. F. Jardim, Phys. Rev. Lett. **94**, 207209 (2005).
[16] J. J. Neumeier, T. Tomita, M. Debessai, J. S. Schilling, P. W. Barnes, D. G. Hinks, and J. D. Jorgensen, Phys. Rev. B **72**, 220505(R) (2005).
[17] H. W. Zandbergen, M. L. Foo, Q. Xu, V. Kumar, and R. J. Cava, Phys. Rev. B **70**, 024101 (2004).
[18] B. C. Sales, R. Jin, K. A. Affholter, P. Khalifah, G. M. Veith, and D. Mandrus, Phys. Rev. B **70**, 174419 (2004).
[19] F. Rivadulla, J.-S. Zhou, and J. B. Goodenough, Phys. Rev. B **68**, 075108 (2003); K. Takada, K. Fukuda, M. Osada, I. Nakai, F. Izumi, Ruben A. Dilanian, K. Kato, M. Takada, H. Rakurai, E. T. Muromachi, and T. Sasaki, J. Mater. Chem. **14**, 1448 (2004).
[20] N. A. Abdullaev, Phys. Solid State **43**, 727 (2001).
[21] B. Yates, *Thermal Expansion* (Plenum Press, New York, 1972), p. 69; T. H. K. Barron and G. K. White, *Heat Capacity and Thermal Expansion at Low Temperatures* (Kluwer Academic, New York, 1999), pp. 144 and 213.
[22] J. Wooldridghe, D. McK Paul, G. Balakrishnan, and M. R. Lees, J. Phys.: Condens. Matter **18**, 4731 (2006).
[23] Y. V. Sushko, O. B. Korneta, S. O. Leontsev, R. Jin, B. C. Sales, and D. Mandrus, cond-mat/0509308 (unpublished).
[24] M. Kund, J. J. Neumeier, K. Andres, J. Markl, and G. Saemann-Ischenko, Physica C **296**, 173 (1998); U. Welp, M. Grimsditch, S. Fleshler, W. Nessler, J. Downey, G. W. Crabtree, and J. Guimpel, Phys. Rev. Lett. **69**, 2130 (1992).
[25] Y.-K. Yu and J. J. Neumeier (unpublished).
[26] D. T. Teaney, Phys. Rev. Lett. **14**, 898 (1965).
[27] M. Tachibana, J. Yamazaki, H. Kawaji, and T. Atake, Phys. Rev. B **72**, 064434 (2005).
[28] H. Kawamura, J. Phys.: Condens. Matter **10**, 4707 (1998).